

## Ammonia-mediated Method for One-step and Surfactant-free Synthesis of Magnetite Nanoparticles

M. Mansournia\*, F. Azizi

Department of Inorganic Chemistry, Faculty of Chemistry, University of Kashan .

### Article history:

Received 15/09/2015

Accepted 10/11/2015

Published online 01/12/2015

### Keywords:

Magnetite

Nanoparticles

Ammonia-mediated method

Superparamagnetic

### \*Corresponding author:

E-mail address:

mansournia@kashanu.ac.ir

Phone: +98 315 5912339

Fax: +98 315 5912397

### Abstract

Magnetite ( $\text{Fe}_3\text{O}_4$ ) nanoparticles have been successfully prepared by a novel one-step and surfactant-free approach utilizing ferrous ion, as a single iron source. In this manner, the reaction occurs between two aqueous solutions via the spontaneous transfer of ammonia gas from one to another in room temperature. No ferric source or oxidizing specie, oxidation controlling and capping agents are needed and the method is suited for large-scale preparation. The effects of reaction conditions on the formation of  $\text{Fe}_3\text{O}_4$  were investigated using powder X-ray diffraction (XRD), Fourier transformation infrared spectroscopy (FT-IR) and scanning electron microscopy (SEM) techniques. The results have demonstrated that the pure and single phase magnetite nanoparticles were synthesized at the final pH values higher than 8. Accordingly, the formation mechanism of these nanostructures is proposed. Moreover, the vibrating sample magnetometry (VSM) measurements of the as-synthesized nanoparticles show their room temperature superparamagnetic characteristic with a typical saturation magnetization of  $51 \text{ emug}^{-1}$ .

2015 JNS All rights reserved

## 1. Introduction

Iron oxides as transition metal oxides, natural minerals and geocatalysts are present in natural aqueous environments and also suspending in aerosols, clouds, and fogs as fine particles [1, 2]. In recent years, the synthesis and utilization of iron oxides nanomaterials have been the subject of intensive scientific curiosity due to their

inexpensive synthesis, easy coating or modification, low toxicity, chemical inertness, biocompatibility and magnetic response [3, 4]. As a result they found potential applications in various fields, particularly in biotechnology and biomedicine, such as drug and gene delivery [5], magnetic resonance imaging [6], tumor therapy and hyperthermia treatment [7].

Magnetite ( $\text{Fe}_3\text{O}_4$ ), maghemite ( $\gamma\text{-Fe}_2\text{O}_3$ ) and hematite ( $\alpha\text{-Fe}_2\text{O}_3$ ) are the most common forms of iron oxides in nature [3]. Magnetite is a member of inverse spinel type ferrites that has exhibited unique electric and magnetic properties based on the transfer of electrons between  $\text{Fe}^{2+}$  and  $\text{Fe}^{3+}$  in the octahedral sites [8]. Accordingly,  $\text{Fe}_3\text{O}_4$  nanostructures are ideal candidates for biomedical [9], catalysis [10] and lithium-ion battery applications [11]. To date various methods have been reported in the literatures for the preparation of ultrafine magnetite nanostructures, such as hydrothermal [12], solvothermal [13], sonochemical [14], electrochemical [15], co-precipitation [16] and oxidative hydrolysis [9]. The present research work focuses on the facile and direct synthesis of  $\text{Fe}_3\text{O}_4$  nanoparticles at room temperature via the ammonia gas-mediated oxidative hydrolysis of  $\text{FeSO}_4$  in the absence of any ferric source or oxidizing specie, oxidation controlling and capping agents. Furthermore, the structural, morphological and magnetic properties of the samples have been studied.

## 2. Experimental procedure

### 2.1. Materials and method

All the chemicals used for experiments were purchased from Merck and used without further purification. In a typical preparation, two beakers, one containing 50 ml of  $\text{FeSO}_4\cdot\text{H}_2\text{O}$  aqueous solution and another 25 ml of the ammonia solution were simultaneously put into a sealed glass container at room temperature for 30 min. After exposure time of  $\text{Fe(II)}$  solution to ammonia gas, the black precipitate was centrifuged, washed several times with distilled water and absolute ethanol, respectively, and then dried at  $70^\circ\text{C}$  in air. In order to understand the influence of the initial concentrations of iron(II) and ammonia on the

structure, purity and morphology of the synthesized nanostructures, six different types of experimental conditions were used by varying the concentrations of  $\text{Fe(II)}$  (0.01M / 0.05M) and ammonia (2M / 5M / concentrated) solutions. In these series of experiments, the initial pH of the reaction media ( $\text{Fe}^{2+}$  solution beaker) was about 3.5 and 8.5-9.5 before and after putting in the ammonia atmosphere, respectively.

### 2.2. Characterization techniques

The initial and final pH values of reaction mixtures were measured using a Metrohm 691 pH meter. The phase structure of the samples was identified by X-ray diffractometer (Philips X'pert Pro X-ray) with Ni-filtered  $\text{Cu K}\alpha$  radiation. Fourier infrared spectra of the products were recorded on a Magna 550 Nicolet spectrophotometer using KBr pellets in the  $400\text{-}4000\text{ cm}^{-1}$  range. The morphology of the as-prepared nanostructures was investigated by the Philips XL-30ESEM and TESCAN VEGA scanning electron microscopes. The magnetization measurements were carried out using a Magnetic Property Measure System (Meghnatis Daghigh Kavir Co.) under magnetic fields up to 10,000 Oe at room temperature.

## 3. Results and discussion

### 3.1. Structural and morphological characterization

The X-ray powder diffraction patterns of three synthesized products obtained by  $\text{FeSO}_4\cdot\text{H}_2\text{O}$  solution as a precursor after exposure to the atmosphere derived from different concentrations of ammonia (2 M, 5 M and concentrated) are shown in Figs. 1a, 1b and 1c, respectively.

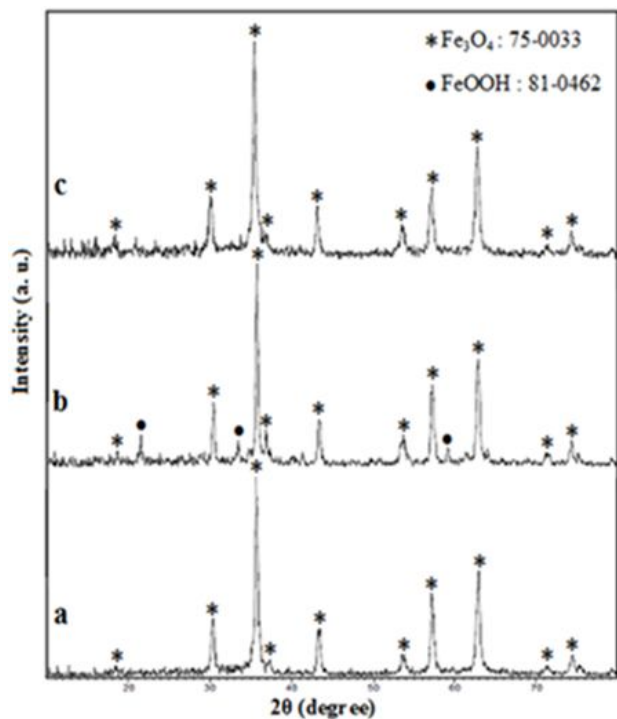


**Fig. 1.** XRD patterns of the samples produced by initial concentrations of Fe(II) and ammonia solutions as: (a) 0.01 M and 2 M, (b) 0.05 M and 5 M, (c) 0.01 M and concentrated, respectively.

The XRD patterns are in good agreement with a cubic structure of  $\text{Fe}_3\text{O}_4$  (space group:  $Fd\bar{3}m$ , JCPDS: 75-0033). The corresponding X-ray reflexes of these three samples in the order of increasing  $2\theta$  can be assigned to the (111), (220), (311), (222), (400), (422), (511), (440), (620) and (533) crystal planes, respectively. However the weak peaks observed at about  $2\theta = 21.4440$ ,  $33.4468$  and  $59.2209$  in Fig. 1b are related to the reflections of orthorhombic phase  $\text{FeOOH}$  (JCPDS card No. 81-0462). The ratio of the integral intensity of these diffraction peaks of  $\text{FeOOH}$  to that of  $\text{Fe}_3\text{O}_4$  is very small, revealing that

magnetite is the major product and the proportion of iron(III) oxyhydroxide is very less in this sample. Moreover, the  $\text{FeOOH}$  peaks disappeared when the  $\text{Fe}^{2+}$  0.01 M solution was used (Figs. 1a and 1c).

On the other hand, a typical FT-IR spectrum of as-formed nanoparticles synthesized using Fe(II) 0.01 M and concentrated ammonia solutions is presented in Fig. 2. The strong minimum at about  $580\text{ cm}^{-1}$  can be assigned to the characteristic of Fe–O stretching mode in the magnetite structure [8, 17]. In addition to this absorption, the bending and stretching vibrations of the weakly bonded water molecules are observed at about  $1630$  and  $3440\text{ cm}^{-1}$ , respectively.

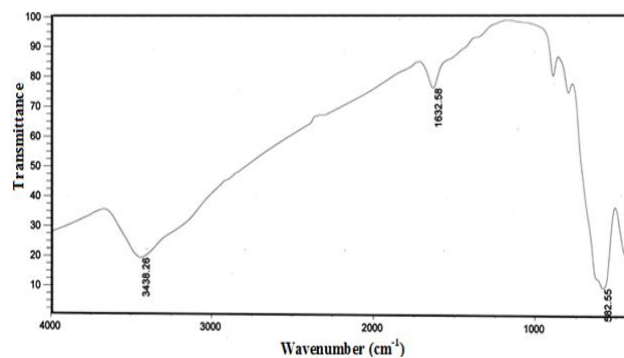


**Fig. 2.** FT-IR spectrum of the sample prepared in the solution of Fe(II) 0.01 M, upon exposure to the atmosphere derived from concentrated  $\text{NH}_3$  solution.

The morphology and particle size of the final products were investigated by SEM images as shown in Fig. 3. It can be seen that the  $\text{Fe}_3\text{O}_4$  nanoparticles are of a diameter in the range of 20–100 nm. Probably, the irregular shape of the nanostructures is due to the rapid nucleation and

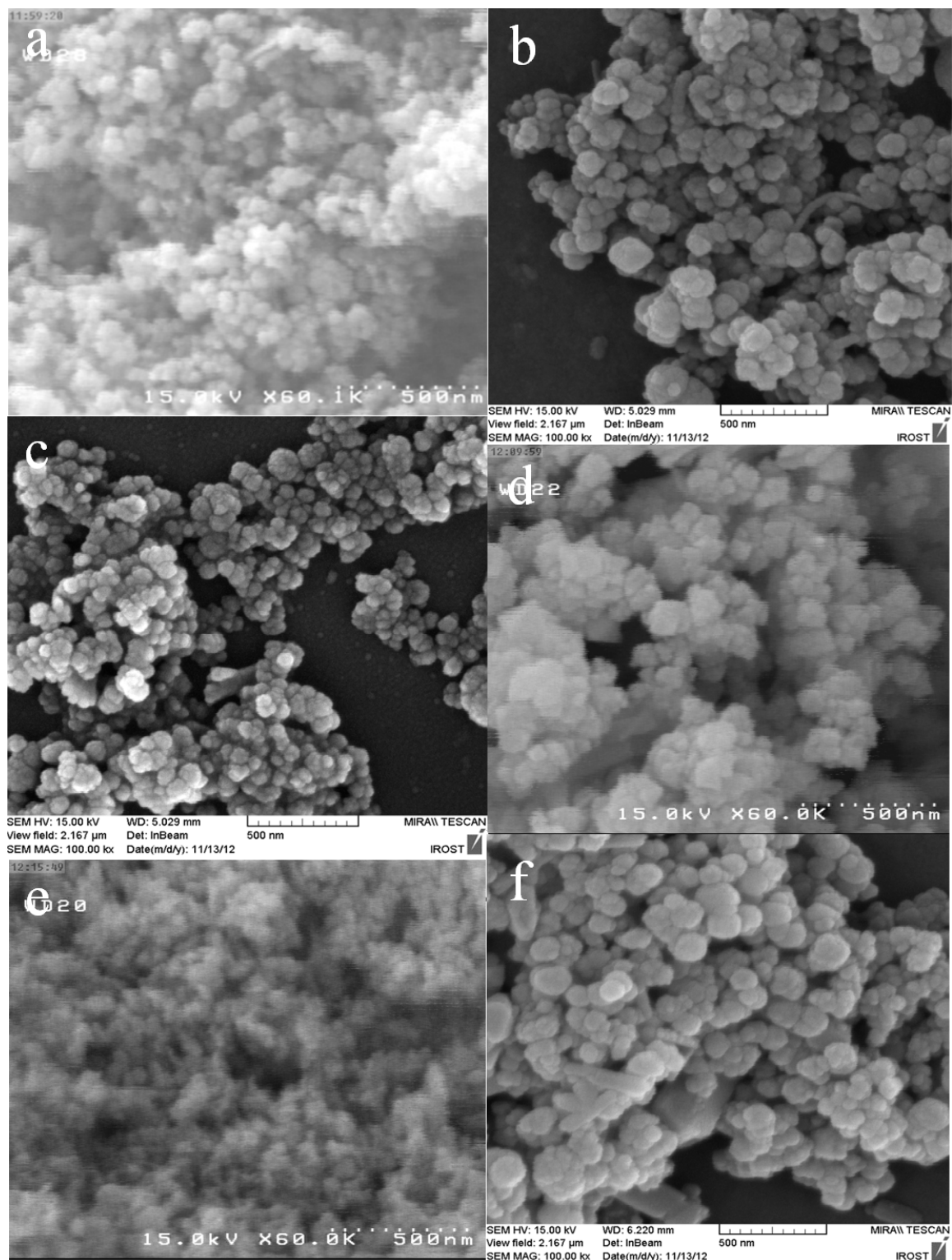


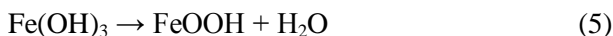
**Fig. 3.** SEM images of the as-prepared magnetite nanoparticles produced by different initial concentrations of Fe(II) and ammonia solutions: (a) 0.01 M and 2 M, (b) 0.05 M and 2 M, (c) 0.01 M and 5 M, (d) 0.05 M and 5 M, (e) 0.01 M and concentrated, (f) 0.05 M and concentrated, respectively.

growth at relatively high pH resulted from the uniform ammonia atmosphere. It is assumed that the excessive NH<sub>3</sub> molecules and OH<sup>-</sup> ions as the capping agents adsorbed on the surface of nanoparticles hinder the Ostwald ripening growth. Therefore, the size of nanoparticles cannot increase significantly.

**3.2. Formation mechanism**

Considering other researchers’ previous studies [12, 13, 18] and our results, the synthesis process of magnetite nanoparticles via the oxidative alkaline hydrolysis of Fe<sup>2+</sup> solution exposure to the ammonia atmosphere is speculated to be as following:

There is a basic solubility of ammonia gas in water to release the hydroxide ions, according to reaction 1. During the synthesis process, the pH value of the Fe<sup>2+</sup> solution reached to at least 8.5, and therefore, OH<sup>-</sup> was first introduced into the Fe<sup>2+</sup> aqueous solution. As a result, colloidal Fe(OH)<sub>2</sub> is formed in reaction 2, which is readily converted to Fe(OH)<sub>3</sub> by oxidation with dissolved oxygen in an alkaline medium (reaction 3). Finally, Fe(II) and Fe(III) hydroxides react together leading to the formation of magnetite (reaction 4). It seems that the negligible amount of FeOOH is obtained in the case of utilizing 0.05 M solution of Fe(II) because no oxidation controlling agent was used in this method, and the excess produced Fe(OH)<sub>3</sub> can be converted to iron(III) oxyhydroxide on the basis of reaction 5.



**3.3. Magnetic characterization**

The vibrating sample magnetometry (VSM) studies distinctly nearly exhibited the superparamagnetic behavior of the as-synthesized magnetite nanoparticles at room temperature because they indicated the hysteresis loop having low remanent magnetization (M<sub>r</sub>) and coercivity (H<sub>c</sub>). Nonetheless, the high saturation magnetization (M<sub>s</sub>) could be resulted in stronger response to an external magnet, which would be extremely useful in various applications. Fig. 4 shows the magnetization curve of the typical Fe<sub>3</sub>O<sub>4</sub> sample which was prepared by initial concentrations of 0.01 M Fe<sup>2+</sup> exposure to the NH<sub>3</sub> atmosphere derived from concentrated ammonia solution. The saturation magnetization value is observed to be 51 emug<sup>-1</sup>. The lack of M<sub>s</sub> value at high fields is a well-know effect due to the small particle size and the high surface area, which lead to some spin canting. It is reported in the literature that the saturation magnetization of magnetite nanoparticles is reduced with decreasing particle size. Therefore, the much smaller M<sub>s</sub> in our case compare to the corresponding value for the bulk magnetite (92 emug<sup>-1</sup>) at room temperature may be assigned to the size, structure and morphology of these nanoparticles [13, 15,17].

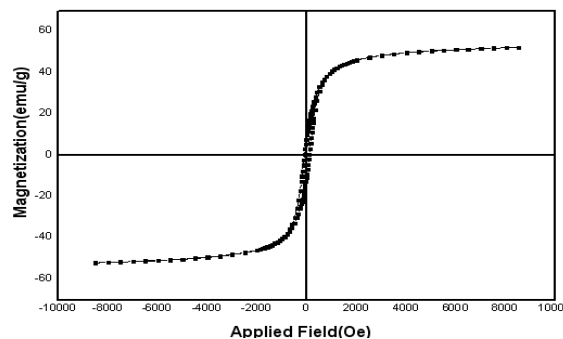


**Fig. 4.** Room temperature M–H curve of typical magnetite nanoparticles obtained from Fe<sup>2+</sup> 0.01 M solution and concentrated ammonia.

#### 4. Conclusion

Magnetite nanoparticles with a diameter in the range of 20-100 nm were successfully prepared by a novel and inexpensive method utilizing the ferrous solution, as a single precursor, exposure to the ammonia atmosphere in a short time and at ambient temperature. Most important of all, this new approach can yield a high purity for Fe<sub>3</sub>O<sub>4</sub> without use of any ferric source or oxidizing specie, oxidation controlling and capping agents. It may also be extended to the synthesis of some other magnetic nanostructures. Additionally, the nano magnetite particles also showed nearly superparamagnetic nature with a saturation magnetization of 51 emug<sup>-1</sup>.

#### Acknowledgment

The authors are grateful to University of Kashan for supporting this work by Grant No 256749/4.

#### References

- [1] R.M. Cornell, U. Schwertmann, *The iron oxides: structure, properties, reactions, occurrences and uses*, second ed., Wiley-VCH, Weinheim, 2004.
- [2] F.B. Li, X.Z. Li, X.M. Li, T.X. Liu, J. Dong, *J. Colloid Interface Sci.* 311 (2007) 481-490.
- [3] P. Xu, G.M. Zeng, D.L. Huang, C.L. Feng, S. Hu, M.H. Zhao, C. Lai, Z. Wei, C. Huang, G.X. Xie, Z.F. Liu, *Sci. Total Environ.* 424 (2012) 1-10.
- [4] J. Joseph, K.K. Nishad, M. Sharma, D.K. Gupta, R.R. Singh, R.K. Pandey, *Mater. Res. Bull.* 47 (2012) 1471-1477.
- [5] W.L. Tung, S.H. Hu, D.M. Liu, *Acta Biomater.* 7 (2011) 2873-2882.
- [6] C. Corot, P. Robert, J. Idee, M. Port, *Adv. Drug Deliv. Rev.* 58 (2006) 1471-1504.
- [7] S. Laurent, S. Dutz, U.O. Hafeli, M. Mahmoudi, *Adv. Colloid Interface Sci.* 166 (2011) 8-23.
- [8] J.H. Li, R.Y. Hong, H.Z. Li, J. Ding, Y. Zheng, D.G. Wei, *Mater. Chem. Phys.* 113 (2009) 140-144.
- [9] J. Murbe, A. Rechtenbach, J. Topfer, *Mater. Chem. Phys.* 110 (2008) 426-433.
- [10] L. Hou, Q. Zhang, F. Jerome, D. Duprez, H. Zhang, S. Royer, *Appl. Catal. B: Environ.* 144 (2014) 739-749.
- [11] D. Su, H. Ahn, G. Wang, *J. Power Sources* 244 (2013) 742-746.
- [12] R. Ramesh, M. Rajalakshmi, C. Muthamizhchelvan, S. Ponnusamy, *Mater. Lett.* 70 (2012) 73-75.
- [13] S. Chaleawlerthumpon, N. Pimpha, *Mater. Chem. Phys.* 135 (2012) 1-5.
- [14] R.V. Solomon, I.S. Lydia, J.P. Merlin, P. Venuvanalingam, *J. Iran Chem. Soc.* 9 (2012) 101-109.
- [15] L. Cabrera, S. Gutierrez, N. Menendez, M.P. Morales, P. Herrasti, *Electrochimica Acta* 53 (2008) 3436-3441.
- [16] Y.K. Jeong, D.K. Shin, H.J. Lee, K.S. Oh, J.H. Lee, D.H. Riu, *Key Eng. Mater.* 317-318 (2006) 203-206.
- [17] F. Chen, Q. Gao, G. Hong, J. Ni, *J. Magn. Magn. Mater.* 320 (2008) 1775-1780.
- [18] R. Fan, X.H. Chen, Z. Gui, L. Liu, Z.Y. Chen, *Mater. Res. Bull.* 36 (2001) 497-502.